AFRL-VA-WP-TP-2004-302

A METHOD FOR ESTIMATING CONTROL FAILURE EFFECTS FOR AERODYNAMIC VEHICLE TRAJECTORY RETARGETING

Michael W. Oppenheimer, David B. Doman, and Michael A. Bolender

FEBRUARY 2004

Approved for public release; distribution is unlimited.

20040331 052

**AIR VEHICLES DIRECTORATE
AIR FORCE RESEARCH LABORATORY
AIR FORCE MATERIEL COMMAND
WRIGHT-PATTERSON AIR FORCE BASE, OH 45433-7542**

REPORT DOCUMENTATION PAGE

1. REPORT DATE *(DD-MM-YY)*	2. REPORT TYPE	3. DATES COVERED *(From - To)*
February 2004	Conference Paper Preprint	

4. TITLE AND SUBTITLE	5a. CONTRACT NUMBER
A METHOD FOR ESTIMATING CONTROL FAILURE EFFECTS FOR AERODYNAMIC VEHICLE TRAJECTORY RETARGETING	In-house
	5b. GRANT NUMBER
	5c. PROGRAM ELEMENT NUMBER N/A

6. AUTHOR(S)	5d. PROJECT NUMBER N/A
Michael W. Oppenheimer, David B. Doman, and Michael A. Bolender	5e. TASK NUMBER N/A
	5f. WORK UNIT NUMBER N/A

7. PERFORMING ORGANIZATION NAME(S) AND ADDRESS(ES)	8. PERFORMING ORGANIZATION REPORT NUMBER
Control Theory Optimization Branch (AFRL/VACA) Control Sciences Division Air Vehicles Directorate Air Force Research Laboratory, Air Force Materiel Command Wright-Patterson AFB, OH 45433-7542	AFRL-VA-WP-TP-2004-302

9. SPONSORING/MONITORING AGENCY NAME(S) AND ADDRESS(ES)	10. SPONSORING/MONITORING AGENCY ACRONYM(S)
Air Vehicles Directorate Air Force Research Laboratory Air Force Materiel Command Wright-Patterson Air Force Base, OH 45433-7542	AFRL/VACA
	11. SPONSORING/MONITORING AGENCY REPORT NUMBER(S) AFRL-VA-WP-TP-2004-302

12. DISTRIBUTION/AVAILABILITY STATEMENT
Approved for public release; distribution is unlimited.

13. SUPPLEMENTARY NOTES
Conference paper to be presented at the AIAA Guidance, Navigation, and Control Conference, Providence, RI, 16-19 August 2004. This material is declared a work of the U.S. Government and is not subject to copyright protection in the United States.

14. ABSTRACT

Advance guidance and control utilizes control reconfiguration, guidance adaptation, trajectory reshaping, and an on-line mission/abort planner to achieve the best possible mission given that the vehicle's performance has been degraded by some sort of failure. Potential failures include actuator loss (locked, floating), engine out, damage to the vehicle, aerodynamic mismodelling, and so on. The trend towards the development of autonomous vehicles has placed more emphasis on requiring trajectory retargeting algorithms. One of the main difficulties of trajectory retargeting is predicting the effects of failures at future flight conditions. In this work, a method is presented that can generate critical information that is required to perform on-line trajectory retargeting.

15. SUBJECT TERMS
Trajectory Retargeting, Trim Constraints, Estimation of Flight Constraints

16. SECURITY CLASSIFICATION OF:			17. LIMITATION OF ABSTRACT:	18. NUMBER OF PAGES	19a. NAME OF RESPONSIBLE PERSON (Monitor)
a. REPORT Unclassified	b. ABSTRACT Unclassified	c. THIS PAGE Unclassified	SAR	16	Michael W. Oppenheimer
					19b. TELEPHONE NUMBER (Include Area Code) (937) 255-8490

i

A Method For Estimating Control Failure Effects For Aerodynamic Vehicle Trajectory Retargeting[*]

Michael W. Oppenheimer [†]

David B. Doman [‡]

Michael A. Bolender [§]

Air Force Research Laboratory, WPAFB, OH 45433-7531

1 Abstract

Advanced guidance and control utilizes control reconfiguration, guidance adaptation, trajectory reshaping, and an on-line mission/abort planner to achieve the best possible mission given that the vehicle's performance has been degraded by some sort of failure. Potential failures include actuator loss (locked, floating), engine out, damage to the vehicle, aerodynamic mismodelling, and so on. The trend towards the development of autonomous vehicles has placed more emphasis on requiring trajectory retargeting algorithms. One of the main difficulties in trajectory retargeting is predicting the effects of failures at future flight conditions. In this work, a method is presented that can generate critical information that is required to perform on-line trajectory retargeting. In particular, a method for estimating failure induced constraints, for failures involving locked or floating control effectors, is presented which accounts for 6 degree-of-freedom (DOF) effects upon the reduced order models that are used by trajectory generation algorithms. These constraints on the vehicle are not constant and can vary widely over different flight conditions. This means that one cannot assume that a set of constraints estimated at a one flight condition will be valid at any other flight condition. This phenomenon limits the class of failures for which one can estimate constraints or 6 DOF effects on reduced order models, using only the original aerodynamic database. Effector failures such as locked or floating surfaces are a class of failures whose effects can be estimated over a wide range of operating conditions. This is because the aerodynamic database for the vehicle does not change as a result of such a failure. The effects of locked or floating surfaces can be estimated at all flight conditions for which the original aerodynamic database is valid. On-line aerodynamic database estimation techniques have not been developed and sensing and identification of outer mold line changes compounds the problem. In order to generate a practical on-line trajectory retargeting algorithm, vehicle constraints must be estimated at future flight conditions and in this

\

work we limit ourselves to dealing with effector failures that can be directly sensed. In this paper, the constraint estimation issue is discussed and brought to the forefront with the use of an example.

2 Introduction

One of the main goals of next-generation reusable launch vehicle technologies is improvement in safety and cost. Under nominal conditions, current guidance and control (G&C) technologies are sufficient for flying a reusable launch vehicle (RLV) into orbit and back to earth for a safe landing and this type of technology has been demonstrated many times.[1] However, it is under failure conditions when advanced guidance and control (AG&C) technologies are most needed. Advanced Guidance and Control (AG&C) technologies are essential for improvements in safety and cost of next-generation launch efforts.[1] AG&C technologies offer the possibility of returning a degraded vehicle safely whenever it is physically possible, without significant ground analysis for each potential failure scenario.

Current AG&C technologies incorporate on-line control reconfiguration and guidance adaptation.[2-4] Here, the available control effectors are used to compensate for a failure as well as recover as much nominal performance as physically possible (also known as inner-loop reconfiguration). When the inner-loop becomes degraded from nominal, guidance loop characteristics may need to be modified so that the inner-loop is not driven into instability. At times, control reconfiguration and guidance adaptation are sufficient to recover a failed vehicle, however, many situations exist where these two efforts are not sufficient.[1,2] Recent analysis of failures on expendable launch vehicles has resulted in the assertion that AG&C technologies would have addressed equivalent failures in an RLV.[1] In the majority of these cases, inner-loop (control) reconfiguration and guidance adaptation would not have been sufficient to recover the failed vehicle. However, the combination of these two techniques along with trajectory retargeting most likely would have recovered the vehicle. Therefore, trajectory retargeting can be used to provide further robustness to vehicle failures by ensuring that a feasible trajectory is available when one exists. Here, when control and guidance reconfiguration are not sufficient, a modified trajectory is computed (or selected) that is feasible and meets, to the extent possible, the mission requirements.

Currently, trajectory retargeting requires a significant amount of ground analysis. Planning for abort and failure situations requires the generation of a large database of feasible trajectories, which in turn requires mass storage and look-ups. These large databases are constructed for a subset of possible failures, however, the large number of failure permutations make it impractical to design trajectories for every failure mode and every flight condition that could be encountered. Also, the time from the start of planning to mission launch can extend for many months. Hence, the turn-around time for a vehicle can be large.

Most of the drawbacks of trajectory retargeting discussed above can be eliminated with the use of on-line trajectory generation, where a new feasible trajectory is computed during flight in response to a failure. On-line trajectory generation has the potential to reduce cost and turn-around time while improving safety. Also, on-line trajectory retargeting is not limited to responding to a set of pre-planned failures.

The computation of retargeted trajectories requires that two major issues be solved:

1. Flight certifiable algorithms must be de-

veloped so that trajectories can be computed on-line.

2. The effects of failures or damage on the vehicle model and vehicle constraints must be quantified.

The contribution of the current work is the development of a method that can estimate the effects of one or more locked or floating control effector failures upon reduced order models used by trajectory retargeting algorithms. In particular, this method can quantify the effects of failures on a vehicle at future flight conditions, providing rotational trim and trim force coefficient information.

This paper is organized as follows. Section 3 details vehicle constraints, Section 4 displays simulation results, while Section 5 contains conclusions. References are also included.

3 Vehicle Constraints

On-board trajectory retargeting or reshaping augments adaptive guidance and reconfigurable control to provide enhanced vehicle robustness to failures. In regards to trajectory retargeting the question becomes: if possible, what trajectory can be flown, given the reduced capability of the vehicle, which will at least safely land the vehicle and at best minimize the deviation from the nominal trajectory? In other words, what is the best feasible trajectory? One difficulty with on-line trajectory reshaping is that the limitations or constraints imposed on the vehicle change with flight condition (Mach number, angle of attack, sideslip, control effector positions). For example, assume a control effector failure occurs on a vehicle during an approach and landing phase of a flight trajectory. At the instant the failure occurs, a trajectory retargeting algorithm could select a feasible trajectory based on the constraints (forces and moments) computed at the current operating condition (Mach number, angle of attack, sideslip, control effector positions). However, as the vehicle progresses further along the flight path, the operating condition changes, resulting in changes to the constraints and vehicle model used for computing the modified trajectory. Hence, a set of commands that are feasible when the failure occurs may not be feasible further along the flight path. In order for the trajectory retargeting algorithm to account for this phenomenon, it is necessary to predict the effects of failures at future operating conditions.

To illustrate the varying nature of reduced order aerodynamic models and constraints, a vehicle, for which an aerodynamic database is available, was selected for this analysis. The vehicle has at its disposal eight control surfaces, right and left outboard elevons, right and left inboard elevons, right and left bodyflaps, and right and left rudders. It is assumed that the sideslip angle $\beta = 0$ and that symmetric flight conditions exist. Therefore, the lateral directional wing-body forces and moments will be assumed to be zero. Thus, only longitudinal motion will be considered.

To begin the analysis, the wing-body pitching moment coefficient of the vehicle is calculated at each data point (j, i) in a grid spanning the eligible regions of the aerodynamic database, giving

$$C_{m_{oj,i}} = f(M_j, \alpha_i) \qquad (1)$$

where $C_{m_{oj,i}} = C_{m_{oj,i}}(M_j, \alpha_i)$ is the base pitching moment coefficient at the jth Mach (M_j) and i^{th} angle of attack (α_i) data point. Since only longitudinal motion is considered here, it is assumed that $C_{rm_{oj,i}}(M_j, \alpha_i) = 0$ and $C_{ym_{oj,i}}(M_j, \alpha_i) = 0$, where $C_{rm_{oj,i}}(M_j, \alpha_i)$, $C_{ym_{oj,i}}(M_j, \alpha_i)$ are the base rolling and yawing moment coefficients at the (j, i) data point, respectively. Now that the wing-body pitching moment has

been computed, a control allocation scheme is used to provide the control effector settings, $\delta_{j,i} \in \mathbb{R}^m$ (m = number of control effectors), that rotationally trim the vehicle. Hence, at each point in the Mach-α envelope, it is desired to find $\delta_{j,i}$ such that

$$
\begin{pmatrix}
C_{rm_{\delta_{j,i}}}(M_j, \alpha_i, \delta_{j,i}) \\
C_{m_{\delta_{j,i}}}(M_j, \alpha_i, \delta_{j,i}) \\
C_{ym_{\delta_{j,i}}}(M_j, \alpha_i, \delta_{j,i})
\end{pmatrix}
=
\begin{pmatrix}
0 \\
-C_{m_{oj,i}}(M_j, \alpha_i) \\
0
\end{pmatrix}
\tag{2}
$$

where $C_{rm_{\delta_{j,i}}}(M_j, \alpha_i, \delta_{j,i})$, $C_{m_{\delta_{j,i}}}(M_j, \alpha_i, \delta_{j,i})$, and $C_{ym_{\delta_{j,i}}}(M_j, \alpha_i, \delta_{j,i})$ are the rolling, pitching, and yawing moment coefficients produced by the control effectors.

All control effectors are position limited so that $\underline{\delta} \leq \delta_{j,i} \leq \overline{\delta}$ where $\underline{\delta}$ and $\overline{\delta}$ are vectors whose elements correspond to the lower and upper limits of the kth control surface. Without loss of generality, locked control effectors are characterized by $\underline{\delta}_k = \overline{\delta}_k$, while floating control effectors are characterized by their lack of moment generating capability, i.e., $C_{rm_{\delta_{j,i}}} = C_{m_{\delta_{j,i}}} = C_{ym_{\delta_{j,i}}} = 0$. We utilize a piecewise linear constrained control allocator[5] to find the appropriate value of $\delta_{j,i}$ which satisfies Equation 2. Let $\delta_{j,i}^*$ denote a solution to Equation 2. If $\delta_{j,i}^*$ can be found such that Equation 2 is satisfied, then sufficient control power exists to longitudinally trim the vehicle. On the other hand, if Equation 2 is not satisfied, then a deficiency exists. By performing this test at each Mach-α point, a rotational trim deficiency map can be constructed. This map indicates where the vehicle is longitudinally trimmable; hence, the map displays trim information for all Mach numbers and angles of attack in the aerodynamic database. In particular, when a point in the deficiency map is zero, then that point is declared longitudinally trimmable; when there is a nonzero value, then a deficiency exists and that point is not trimmable. Thus, from this information, one can determine the range of trimmable angle of attack. This range provides information on vehicle constraints imposed by a failure, that is, given a Mach number, the vehicle can only fly at an angle of attack for which it can be rotationally trimmed.

Similar to generating the trim deficiency map, trim force coefficient maps can be created. These maps provide the drag and lift at every operating condition for which a model is available. The lift and drag can be computed at each operating point by substituting the solution to Equation 2, $\delta_{j,i}^*$, into the aerodynamic database and calculating the trim lift and drag coefficients. The total lift and drag coefficients are given by the sum of the wing-body and control surface coefficients for a given Mach-α pair and corresponding $\delta_{j,i}^*$:

$$
\begin{aligned}
C_L(M_j, \alpha_i) &= \\
C_{L_o}(M_j, \alpha_i) + C_{L_{\delta_{j,i}^*}}&(M_j, \alpha_i, \delta_{j,i}^*) \\
C_D(M_j, \alpha_i) &= \\
C_{D_o}(M_j, \alpha_i) + C_{D_{\delta_{j,i}^*}}&(M_j, \alpha_i, \delta_{j,i}^*)
\end{aligned}
\tag{3}
$$

where $C_L(M_j, \alpha_i)$ and $C_D(M_j, \alpha_i)$ are the total lift and drag coefficients, $C_{L_o}(M_j, \alpha_i)$ represents the wing-body lift coefficient, $C_{D_o}(M_j, \alpha_i)$ represents the sum of the wing-body induced and parasitic drag coefficients, and $C_{L_{\delta_{j,i}^*}}(M_j, \alpha_i, \delta_{j,i}^*)$, $C_{D_{\delta_{j,i}^*}}(M_j, \alpha_i, \delta_{j,i}^*)$ are the sum of the lift and drag coefficients produced by the control effectors, respectively.

The algorithm to compute pitch deficiency, drag, and lift maps and to determine the range of trimmable angle of attack is summarized as follows:

4

1. Define a grid for Mach and Angle of Attack, including lower and upper bounds and step size

2. Initialize δ

3. Loop 1 → For j = 1 to Number of Machs

4. Loop 2 → For i = 1 to Number of Angle of Attacks

5. Compute the wing-body pitching moment coefficient, $C_{m_{oj,i}}(M_j, \alpha_i)$

6. Solve a control allocation problem to find $\delta_{j,i}^*$ which satisfies Equation 2

7. Compute trim deficiency at each point, i.e., deficiency(j,i) =

$$\left\| \begin{bmatrix} 0 \\ -C_{m_{oj,i}}(M_j, \alpha_i) \\ 0 \end{bmatrix} - \begin{bmatrix} C_{rm_{\delta j,i}}(M_j, \alpha_i, \delta_{j,i}) \\ C_{m_{\delta j,i}}(M_j, \alpha_i, \delta_{j,i}) \\ C_{ym_{\delta j,i}}(M_j, \alpha_i, \delta_{j,i}) \end{bmatrix} \right\|_2$$

8. If deficiency(j,i) = 0, then the corresponding Mach-α combination is trimmable

9. Compute drag and lift at each data point by substituting $\delta_{j,i}^*$ into the aerodynamic database

10. Increment Mach and/or Alpha

11. End Angle of Attack loop

12. End Mach loop

This algorithm yields the control deficiency map as well as the lift and drag maps. Each map is valid for all operating conditions for which a model is available.

4 Results

In this section, some of the aforementioned maps will be displayed for both un-failed and failed cases. In particular, rotational trim deficiency maps, which provide the range of trimmable angle of attack, and drag and lift maps will be shown.

As an example, we consider a reentry vehicle with left/right inboard elevons, left/right outboard elevons, left/right bodyflaps, and left/right ruddervators. The vehicle's aerodynamic database covers a wide range of conditions, from Mach 5 to Mach 0.3 and over an angle of attack range of $-10°$ to $50°$. The technique described in Section 3 is used to compare the trim maps and trim force coefficients of the nominal vehicle to those of a failed vehicle.

To begin, consider the nominal vehicle. Figure 1 displays the rotational trim deficiency map for the un-failed vehicle. It is easily discernable that there are no combinations of Mach-α for which the vehicle is not statically longitudinally trimmable, as all of the deficiency values are quite small. As expected from the deficiency map in Figure 1, the range of trimmable angle of attack is $-10°$ to $50°$ for all Mach numbers, since there are no locations which display rotational trim deficiency. Figure 2 displays the pitch deficiency map for a failure of both bodyflaps at $26°$. Figure 2 immediately portrays the feasible range of angle of attack (angle of attack values for which the trim deficiency map is zero). For a trajectory which would span the entire Mach range shown here, it can be seen that the range of feasible angle of attack is much smaller than the range of the nominal case. In fact, the feasible region of angle of attack and Mach number reduces to a corridor on the Mach-α grid, as illustrated in Figure 3. This corridor corresponds to angle of attack values which are less than about $3°$. For low Mach numbers,
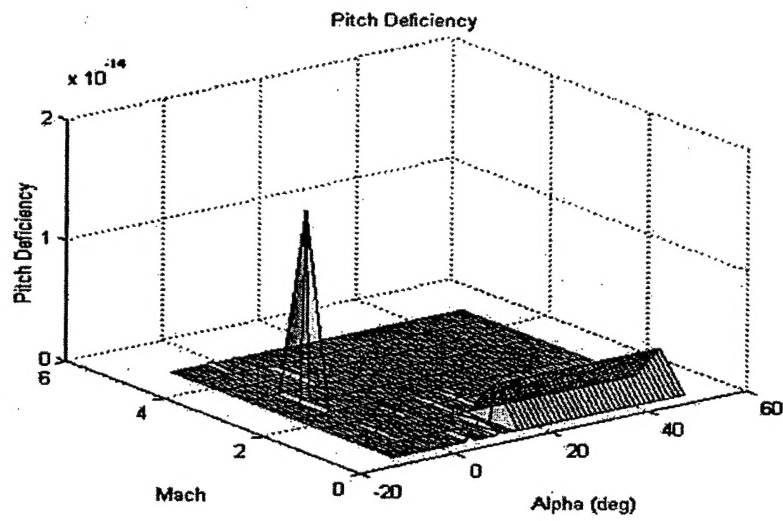
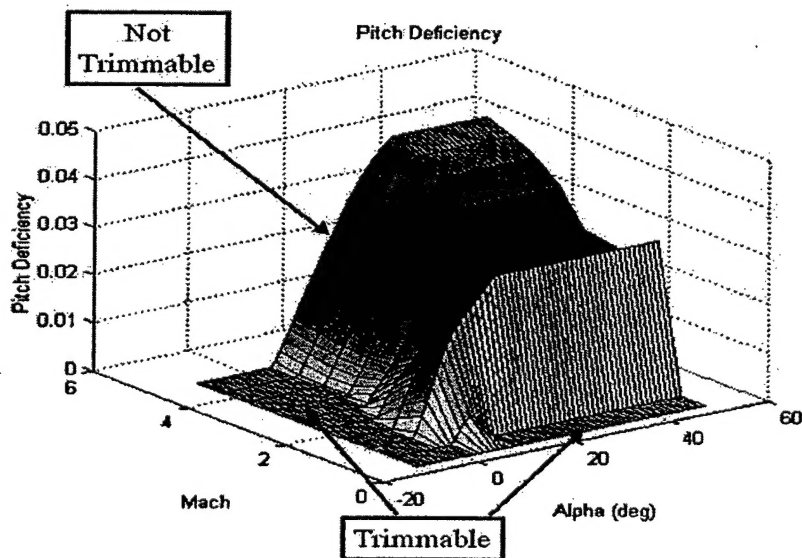Figure 1: Pitch Deficiency For Nominal Vehicle.

Figure 2: Pitch Deficiency For Failed Left and Right Body Flaps at 26°.
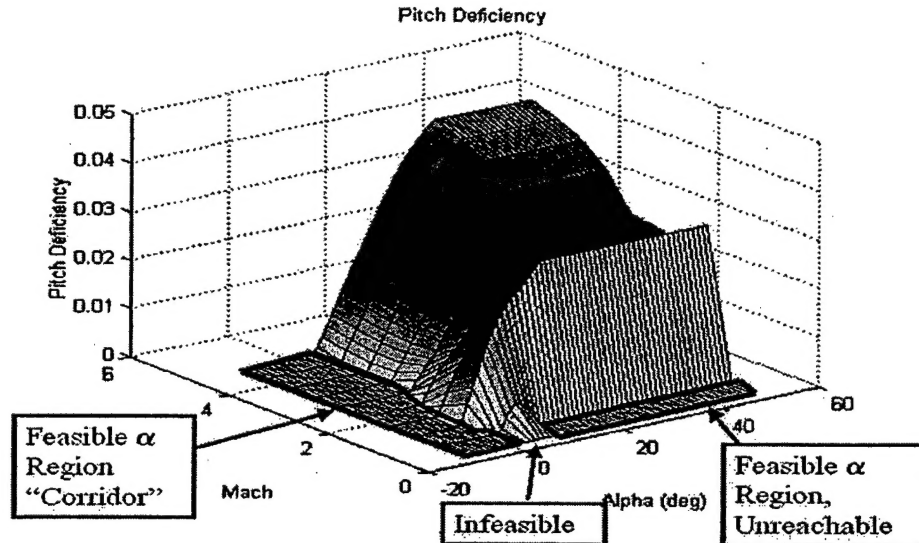
6

Figure 3: Pitch Deficiency: Feasible α Corridor And Unreachable Regions.

higher angle of attack values are permissable, however, because there is a small region of infeasibility at low Mach numbers (between 3° and 7° angle of attack), the vehicle can never obtain these larger α values (see feasible α region, unreachable in Figure 3). Once the trim deficiency map has been created, a simple interpolation scheme can be used to define the boundary between the trimmable and non-trimmable regions. In this way, one can determine the range of trimmable angle of attack for all Mach numbers of interest.

Now, the trim force coefficients will be investigated. Figures 4 and 5 display the drag and lift coefficients for the un-failed and failed cases. These figures show how failures can affect the drag and lift characteristics of a vehicle. As can be seen in Figure 4, there are regions where the drag changes significantly. On the other hand, Figure 5 shows that the lift is not significantly influenced by the failure. In general, changes in drag and lift, due to control surface failures, are strongly dependent on the vehicle. As a rule, the larger the control effectors are with re-

spect to the wing-body, the greater the impact a failure will have on the force model. A smaller vehicle with large, powerful control surfaces would display larger changes in drag and lift. Figures 6 and 7 illustrate the effect of a failure upon the drag and lift forces for a re-entry vehicle where the sizes of the control surfaces are relatively large. This vehicle has at its disposal 6 control effectors: left/right flaperons, left/right ruddervators, a speedbrake, and a bodyflap. Here, it is easily discernable that the failure of both ruddervators at 5° has caused a large change in drag and lift as compared to the nominal case. For this vehicle, the ruddervators are extremely powerful and hence, large changes in drag and lift are observed.

One of the key points to all of this is that the failure induced constraints, be it trimmable angle of attack, drag, or lift are not constant from one flight condition to another. For example, consider Figure 2. Assume that at Mach 5 during a flight, both bodyflaps fail at 26°. If an algorithm were to compute the range of trimmable angle of
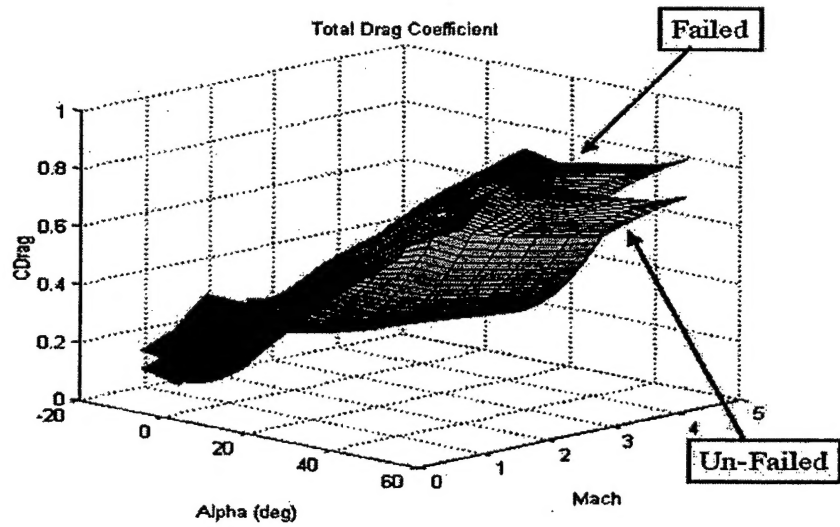
7

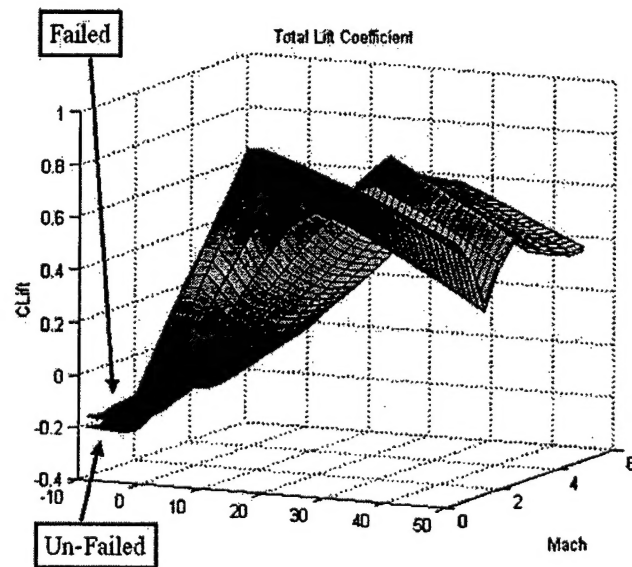Figure 4: Drag Coefficient For Failed And Un-Failed Configurations.

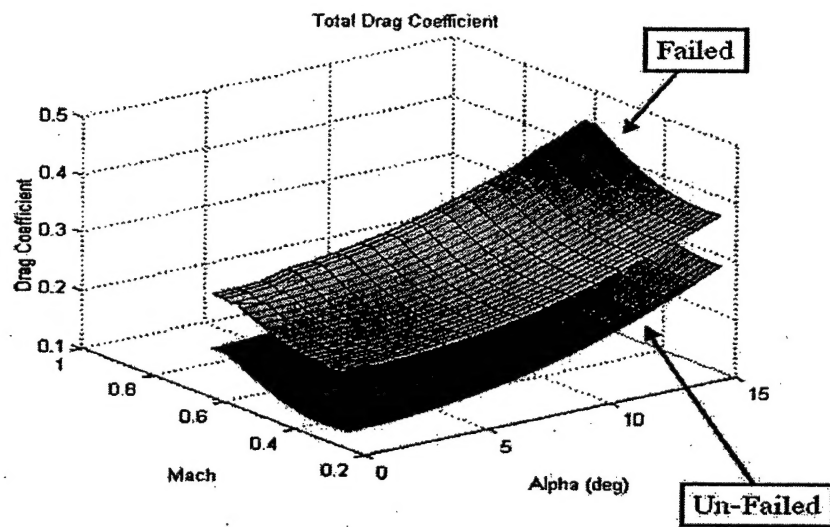Figure 5: Lift Coefficient For Failed And Un-Failed Configurations.

8

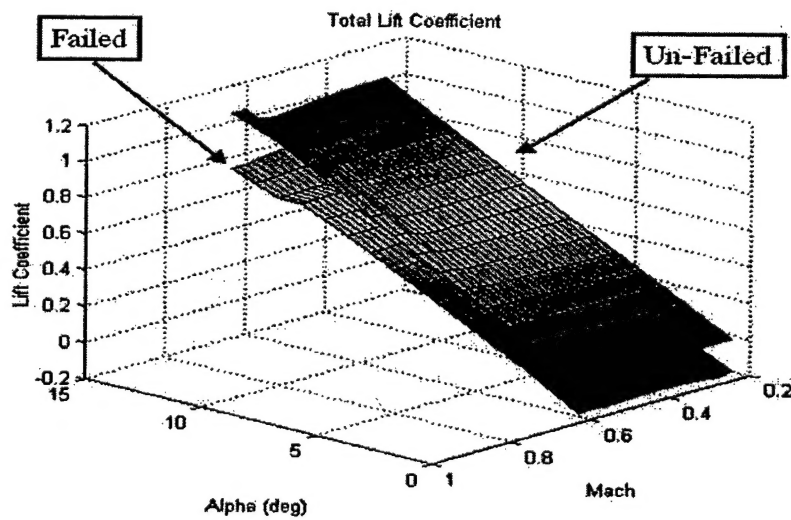Figure 6: Drag Coefficient For A Vehicle Whose Control Surfaces Are Large Relative To The Wing-Body.

Figure 7: Lift Coefficient For A Vehicle Whose Control Surfaces Are Large Relative To The Wing-Body.

attack at that instant, the range would be from $-10°$ to about $3°$. Typically, this information would be used by a trajectory retargeting algorithm to compute a new trajectory to finish the mission. However, this information is not sufficient for a trajectory retargeting algorithm because the range of trimmable angle of attack is not constant. As seen in Figure 2, from Mach 2.5 to Mach 0.5, the range of trimmable angle of attack shrinks to about $-10°$ to $-2°$. Hence, the effects of failures, at future flight conditions can change and must be computed for use in a retargeting algorithm. The procedure developed in this work allows calculation of the effects of failures at every flight condition defined in the aerodynamic model. Coupling the range of trimmable angle of attack with drag and lift maps for a full-envelope of operating conditions provides a trajectory retargeting algorithm the information required to compute a feasible trajectory, if possible, throughout the remaining flight regime, given the vehicle's limitations.

5 Conclusions

One of the main difficulties in trajectory retargeting is predicting the effects of failures at future flight conditions. In this paper, a method to predict the drag and lift characteristics of a vehicle under locked or floating control effector failures was described. The method also provides a means of determining regions of the flight envelope where the vehicle can be rotationally trimmed, by creating a rotational trim deficiency map. Locations where the trim deficiency map are non-zero indicate regions of non-trimmable angle of attack/Mach number, while zero values for the deficiency map indicate regions of rotationally trimmable angle of attack/Mach number. Hence, if a failure is identified in flight, deficiency, drag, and lift maps can be computed quickly using the technique de-

scribed in this work. Once this information is available, trajectory retargeting algorithms have access to the feasible range of angle of attack and well as the drag and lift models at all feasible flight conditions. Thus, the retargeted flight path can be restricted to obey the angle of attack and drag and lift limitations available in these maps.

References

[1] J. M. Hanson, "New guidance for new launchers," *Aerospace America*, vol. 41, no. 3, pp. 36–41, March 2003.

[2] J. D. Schierman, J. R. Hull, and D. G. Ward, "Adaptive Guidance With Trajectory Reshaping For Reusable Launch Vehicles," in *Proceedings of the 2002 Guidance, Navigation and Control Conference*, AIAA 2002-4458, August 2002.

[3] B. Kim and A. Calise, "Nonlinear flight control using neural networks," *Journal of Guidance, Control and Dynamics*, vol. 20, no. 1, pp. 26–33, 1997.

[4] M. W. Oppenheimer and D. B. Doman, "Reconfigurable Control Design For The X-40A With In-Flight Simulation Results," in *Proceedings of the 2004 Guidance, Navigation and Control Conference*, AIAA 2004-xxxx, August 2004.

[5] M. Bolender and D. B. Doman, "Nonlinear control allocation using piecewise linear functions," in *Proceedings of the 2003 Guidance, Navigation and Control Conference*, AIAA 2003-5357, August 2003.